ICE CAPS UNDER SAND CAPS UNDER AN ICE CAP: REVEALING A RECORD OF CLIMATE CHANGE ON MARS WITH SHARAD S. Nerozzi[1] and J. W. Holt[1], [1]Institute for Geophysics, Jackson School of Geosciences, The University of Texas at Austin (stefano.nerozzi@utexas.edu, holt@utexas.edu)

Introduction: The cavi unit is an aeolian deposit of sand and water ice making up a large fraction of Planum Boreum in the northern hemisphere of Mars [1-8]. Ref. [5,7] determined an age for this unit of 10-100 Ma. Its stratigraphic position between the underlying rupes unit (cavi and rupes together comprise what is termed the "basal unit," BU, [3]) and the overlying, nearly pure water-ice north polar layered deposits (NPLD) implies that its strata record regional and global climate conditions and processes in middle-late Amazonian during a global climate transition.

Prior studies involving imagery, spectrometry and radar sounding determined that the cavi unit is composed of a mixture of water ice and lithic materials [1-8]. However, there is still no consensus on its precise composition, and it remains unclear which fraction, water ice or sand, dominates. Precise constrains on composition are needed to determine the importance of the cavi unit as a water and sediment reservoir, reconstruct its accumulation history and understand the climatic and other processes that resulted in its observable morphology and stratigraphy.

Profiles acquired by the Shallow Radar (SHARAD, [9]) reveal a deep reflector within Planum Boreum, generally located in regions where no rupes unit is present. We associate this reflector with the basal contact of the cavi unit with the underlying Vastitas Borealis interior unit (Hbvi, [7]). We use an inversion technique to determine the dielectric constant (real part of dielectric permittivity) of this unit and, in turn, its bulk composition.

Methods: We identify and trace the top and basal reflectors of the cavi unit within SHARAD profiles, and export the time delay information associated with each of these surfaces. The elevation of the upper surface of the cavi unit is determined by removing the thickness of the overlying NPLD where present, assuming a bulk composition of water ice (ε'=3.1, [10]), or directly derived from Mars Orbiter Laser Altimeter (MOLA, [11]) digital elevation model where the unit is exposed. The cavi unit basal elevation is derived by interpolating the surrounding Hbvi unit MOLA shotpoints and SHARAD-derived elevations with a 6th degree polynomial. The dielectric constant is then calculated with:

$$\varepsilon' = \left(\frac{tc}{2h}\right)^2$$

where t is the two-way time delay between the top and basal surfaces, c is the speed of light in vacuum, and h is the thickness of the unit. Then, we can estimate the bulk composition as mixture of basalt (ε'=8.8, [12]),

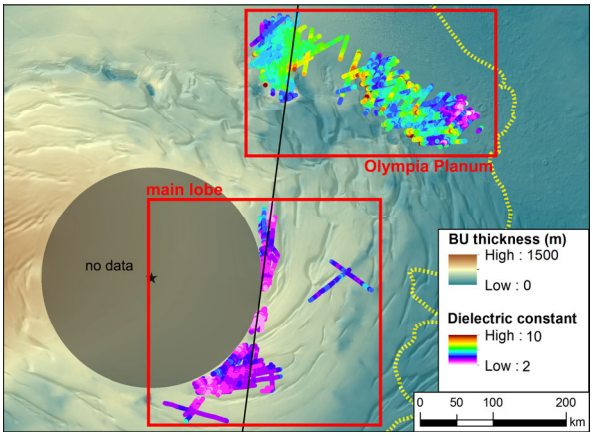

Figure 1: Map of computed dielectric constant across Planum Boreum, with superimposed topographic shaded relief of the modern surface. The black line delineates the location of profile 1294501 in Fig. 2.

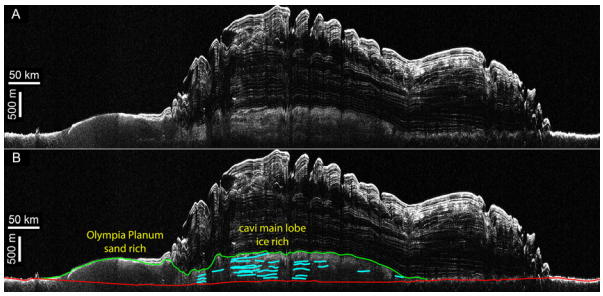

Figure 2: (a) SHARAD profile 1294501 depth corrected assuming bulk water ice composition (e=3.1 [10]), and (b) interpretation of reflectors within cavi (blue). The putative basal surface of cavi (top of Hbvi unit) is represented in red.

gypsum (ε'=5.4, [13], hypothesized to be present within cavi [14]) and water ice (ε'=3.1, [10]) by contructing a ternary diagram based on a mixing power law:

$$\varepsilon'_{mix}{}^{1/\gamma} = \sum \phi_{comp} \varepsilon'_{comp}{}^{1/\gamma}$$

where γ=2.7 for ice and sand mixtures [15] and ϕ_{comp} is the component fractional volume. We assume that the lithic components, basalt and gypsum, make up the sand grains and water ice fills in the intergranular pore space (i.e. no air is present).

Results: Our exercise reveals that the bulk dielectric constant of the cavi unit has substantial spatial variability (Fig. 1). We therefore decided to divide the unit into two study areas, Olympia Planum and the main lobe.

Olympia Planum is covered by the largest dune field on Mars, and cavi makes up most of the volume underneath [5]. SHARAD detects a deep reflector in the eastern end of Olympia Planum that we interpret as its basal surface (Fig. 2). No other reflectors were identified in

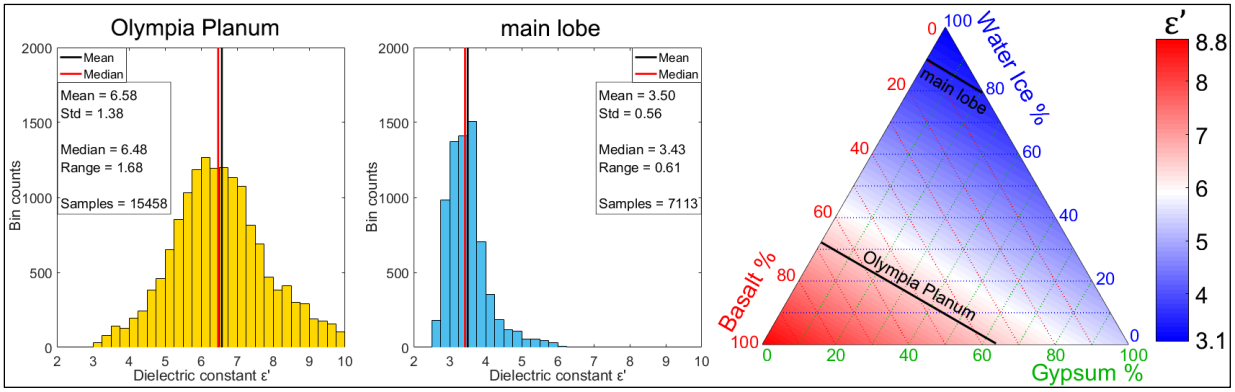

Figure 3: (left) Dielectric constant distribution in the two study areas, and (right) the average dielectric constant of both locations plotted in a ternary diagram based on a mixing power law with a mixture of basalt, gypsum and water ice.

Olympia Planum. We determine a bulk dielectric constant ε'=6.58 (Fig. 3). The distribution and trending values are very similar to those obtained by ref. [16] (for the cavi surface in Boreales Scopuli using SHARAD).

Several reflectors appear in the cavi unit main lobe (Fig. 2). We interpret the lowermost of these as the base of the cavi unit. Here the dielectric constant distribution has a positively skewed normal distribution with a mean ε'=3.50 (Fig. 3). Assuming a two-component basalt and water ice mixture, we calculate a bulk composition dominated by water ice with only ~10% siliciclastic impurities by volume. This result is compatible with the results of ref. [6], who found that the BU composition is qualitatively similar to that of the NPLD based on MARSIS data.

Discussion: The dielectric constant inversion results indicate that the two regions of cavi unit have remarkably different compositions. Olympia Planum bulk dielectric constant is equivalent to a mixture of 68% basaltic sand and 32% water ice, which corresponds to the low end of typical aeolian sand porosities [17]. We find plausible that a minor fraction of the water ice makes up thin layers and lenses within the sandy deposits, as observed across most visible cavi outcrops. Ggypsum may also make up a small fraction of the lithic component, but its presence is not necessary to explain our results.

In the main lobe, water ice appears to be the dominant fraction at 80-90%, but exceeds by far the maximum observed porosity of aeolian sand deposits (50%, [17]), even assuming an implausible mixture of water ice and pure gypsum. We note that compared to Olympia Planum, the cavi unit main lobe is crossed by several internal reflectors (Fig. 2), which indicates the presence of a similar number of significant changes in composition. Based on this qualitative observation, and the decrease in dielectric constant with increasing thickness and latitude, we hypothesize that the main lobe is made of alternating sandy and pure water ice layers.

Several water ice accumulation models predict substantial water ice accumulation during periods of low spin axis abliquity before the onset of the NPLD [18,19], with the thickest accumulation at higher latitudes. These are soon followed by complete loss by sublimation. We hypothesize that some of this ice has been buried and preserved by aeolian sand sheets that prevented complete sublimation. Similar sand mantles extending for 10s of km have been observed on top of thick water ice [20], and within the lowermost NPLD [5, 21]. Therefore, we argue that previously accumulated ice caps are not necessarily lost during high obliquity periods, but preserved within sand sheets underneath the NPLD. These ice deposits are detected by SHARAD and can be delineated in their spatial extent. Moreover, the high water ice fraction makes cavi an important water ice reservoir, potentially the third largest on Mars after the two PLDs.

Acknowledgments: This work was supported by NASA MDAP grant NNX15AM52G.

References: [1] Byrne S. and Murray B.C. (2002) *JGR, 107*, 11-1-11-2. [2] Edgett K.S. et al. (2003) *Geomorph., 52*, 289-297. [3] Fishbaugh K.E. and Head J.W. (2005) *Icarus, 174*, 444–474. [4] Phillips R.J. et al. (2008) *Science, 320*, 1182-1185. [5] Tanaka K.L. et al. (2008) *Icarus, 196*, 318–158. [6] Selvans M.M. et al. (2010) *JGR, 115*, E09003. [7] Tanaka K.L. and Fortezzo C.M. (2012) *https://pubs.usgs.gov/sim/3177/* [8] Brothers T.C. et al. (2015) *JGR, 120*, 1357–1375. [9] Seu R. et al. (2007b) *JGR, 112*, E05S05. [10] Grima C. et al. (2009) *GRL, 36*, L03203. [11] Smith D.E. et al. (2001) *JGR, 106*, 23689-23722. [12] Nunes D.C. and Phillips R.J. (2006) *JGR, 111*, E06S2. [13] Heggy et al. (2001) *Icarus, 154*, 244-257. [14] Massé M. et al. (2012) *EPSL, 317-318*, 44-55. [15] Stillman D.E. et al. (2010) *J. Phys. Chem. B, 114*, 6065-6073. [16] Lauro S.E. et al. (2012) *Icarus, 219*, 458-467. [17] Pye K. and Tsoar K. (2008), 74-89. [18] Levrard B. et al. (2007) *JGR, 112*, E06012. [19] Greve R. et al. (2010) *PSS, 58*, 931-940. [20] Conway S.J. et al. (2012) *Icarus, 220*, 174-193. [21] Nerozzi N. and Holt J.W. (2017) *LPSC XLVII, Abstract #1722.*